Journal of Marine Systems 158 (2016) 93–105

Contents lists available at ScienceDirect

Journal of Marine Systems

journal homepage: www.elsevier.com/locate/jmarsys

A survey of the summer coccolithophore community in the western Barents Sea

Jacques Giraudeau [a,*], Vivien Hulot [b], Vincent Hanquiez [a], Ludovic Devaux [a], Hélène Howa [b], Thierry Garlan [c]

[a] Université Bordeaux, CNRS, EPHE, UMR 5805 EPOC, Allée Geoffroy Saint-Hilaire, CS 50023, 33615 Pessac Cedex, France
[b] Université Angers, CNRS, UMR 6112 LPG-BIAF, Faculté des Sciences, 2 boulevard Lavoisier, 49045 Angers Cedex 1, France
[c] SHOM, Service Hydrographique et Océanographique de la Marine, 13 rue du Chatellier, 29200 Brest, France

ARTICLE INFO

Article history:
Received 27 August 2015
Received in revised form 17 February 2016
Accepted 29 February 2016
Available online 2 March 2016

Keywords:
Coccolithophores
Western Barents Sea
Summer phytoplankton community
Coccolith calcite

ABSTRACT

The Barents Sea is particularly vulnerable to large-scale hydro-climatic changes associated with the polar amplification of climate change. Key oceanographical variables in this region are the seasonal development of sea-ice and the location and strength of physico-chemical gradients in the surface and subsurface water layers induced by the convergence of Arctic- and Atlantic-derived water masses. Remote sensing imagery have highlighted the increasing success of calcifying haptophytes (coccolithophores) in the summer phytoplankton production of the Barents Sea over the last 20 years, as a response to an overall larger contribution of Atlantic waters to surface and sub-surface waters, as well as to enhanced sea-ice melt-induced summer stratification of the photic layer.

The present study provides a first thorough description of coccolithophore standing stocks and diversity over the shelf and slope of the western Barents Sea from two sets of surface and water column samples collected during August–September 2014 from northern Norway to southern Svalbard. The abundance and composition of coccolithophore cells and skeletal remains (coccoliths) are discussed in view of the physical–chemical–biological status of the surface waters and water column based on in-situ (temperature, salinity, fluorescence) and shore-based (microscope enumerations, chemotaxonomy) measurements, as well as satellite-derived data (Chl *a* and particulate inorganic carbon contents).

The coccolithophore population is characterized by a low species diversity and the overwhelming dominance of *Emiliania huxleyi*. Coccolithophores are abundant both within the well stratified, Norwegian coastal water — influenced shallow mixed layer off northern Norway, as well as within well-mixed cool Atlantic water in close vicinity of the Polar Front. Bloom concentrations with standing stocks larger than 4 million cells/l are recorded in the latter area north of 75°N. Our limited set of chemotaxonomic data suggests that coccolithophores contribute substantially (ca. 20% of the total Chl *a*) to the summer phytoplankton community which is made essentially of small-sized algal groups. Excluding the bloom area, coccolith calcite accounts for an average of 20% to the bulk particulate inorganic carbon content in the surface waters, and explains to some extent the satellite-derived spatial distribution of this parameter. Deep water living coccolithophore species thriving below the pycnocline as well as populations present in well-mixed cool Atlantic water are rapidly transferred to depth in the form of intact coccospheres down to at least 200 m. High amplitude internal waves which, according to our observations, affect a wide range of water depth up to the lower photic zone, might strengthen the vertical transfer of this sinking population.

1. Introduction

The hydrology of the shallow marginal Barents Sea contributes, together with the ocean circulation over Fram Strait, to the water mass exchanges between the Arctic and the Atlantic Oceans. Strong winds and convective overturning in winter, input of warm, nutrient rich Norwegian Atlantic Water (NwAW), and seasonal sea-ice melting combine to trigger an extensive spring bloom in the Barents Sea, with Chlorophyll *a* (Chl *a*) concentrations (a proxy for phytoplankton biomass) typically ranging from 2 to 10 mg/m^3 (Signorini and McClain, 2009). These values are among the highest recorded at the scale of the Arctic Ocean realm (Hunt and Drinkwater, 2005). Satellite imagery (Smyth et al., 2004; Burenkov et al., 2011) highlighted a profound change in phytoplankton dynamics and functional groups in surface waters of the Barents Sea over the last 25 years, a change which is characterized by the recurring development of extensive blooms of the coccolithophore *Emiliania huxleyi* during summer. This species reaches maximum concentrations in August, within a wide area of

---

[*] Corresponding author. Tel.: +33 5 40 00 88 60.
E-mail address: jacques.giraudeau@u-bordeaux.fr (J. Giraudeau).

http://dx.doi.org/10.1016/j.jmarsys.2016.02.012
0924-7963/

stratified, nutrient-depleted surface waters of the central and southern Barents Sea (Signorini and McClain, 2009). This phenomenon is part of the present general poleward expansion of *E. huxleyi* as reviewed by Winter et al. (2014). In the Barents Sea, it tends to extend nowadays further north, though with lower cell concentrations, along the Eurasian shelf break off Eastern Svalbard (Hegseth and Sundfjord, 2008). The contribution of the calcifying *E. huxleyi* to the high summer concentrations of particulate inorganic carbon (PIC) in surface waters of the central and southern Barents Sea has been testified by in-situ sampling and microscope observations of coccolithophore populations (Smyth et al., 2004). The most recent microscope observations of water samples collected within the central Barents Sea along 30°E and located within an area of high surface water backscattering from remote sensing observations, revealed coccolithophore concentrations ranging from 2 to 20 million cells/L (Burenkov et al., 2011; Hovland et al., 2014). The recent summer development of coccolithophore blooms in the Barents Sea has been related to the polar amplification of recent climate change which translates into positive temperature anomalies (increasing AW influence) and negative salinity anomalies (increasing seasonal sea-ice melting) (Smedsrud et al., 2013). Both anomalies act for the summer setting of a highly stratified photic layer (Smyth et al., 2004), the mixed layer depth (MLD) shoaling to a mean value of 10 m within the southern Barents Sea where coccolithophore blooms are the most frequently recorded (Signorini and McClain, 2009). This modern modification of phytoplankton dynamics and species groups potentially contributes to the on-going changes in the dynamics of higher trophic levels in the Barents Sea, from zooplankton to pelagic fish stocks (Dalpadado et al., 2012).

The present study provides a first thorough description of coccolithophore standing stocks and diversity in the western Barents Sea shelf and slope during the summer peak production period of this floral group in 2014. The abundance and composition of coccolithophore cells and skeletal remains (coccoliths) in surface and water column samples are discussed in view of the physical–chemical–biological status of the photic layer. Beside describing and understanding the bulk and species level pattern of coccolithophore distribution, we aim here at providing key information on the contribution of these calcareous prymnesiophytes to the summer phytoplankton population and surface water PIC within this polar region.

2. Oceanographic setting

The surface and intermediate circulation of the Barents Sea is characterized by the opposing flow of Atlantic and Arctic waters whose boundary is defined by the Polar Front (PF) (Fig. 1). The location of the PF in the western Barents Sea is closely controlled by the bottom topography and displays a meandering pattern steered by the bathymetrically shallow Spitsbergenbanken and the Storfjorden and Bjørnøyrenna glacial troughs (Loeng, 1991; Ozhigin et al., 2000). The North Cape Current (NCC), an extension of the Norwegian Atlantic Current (NwAC), which carries the main flow of Atlantic water into the Barents Sea, circulates over the latter, more extended trough. Further north along the Barents Sea margin and western Svalbard slope, the poleward flow of Atlantic water to Fram Strait is carried by the West Spitsbergen Current. The southward flowing East Spitsbergen Current and Persey Current transport cold and fresh polar waters to the central and western Barents Sea and merge over the Spitsbergenbanken to form the Bjørnøya Current (Loeng, 1991).

3. Material and methods

Surface and water column sampling took place as part of the marine geological and geophysical cruise MOCOSED 2014 of the French *Service Hydrographique and Oceanographique de la Marine* (SHOM) on-board the RV *Pourquoi Pas*? during August–September 2014. The investigated area covers the western Barents Sea shelf and slope from northern Norway to southern Svalbard (Fig. 1).

3.1. Oceanographic data

The environmental dataset is based on the integration of underway measurements, data obtained from multisensor vertical casts at CTD stations, and remote sensing imagery.

Sea-surface temperatures (SSTs) and salinities (SSSs) were measured at each underway coccolithophore sampling station (×50) from

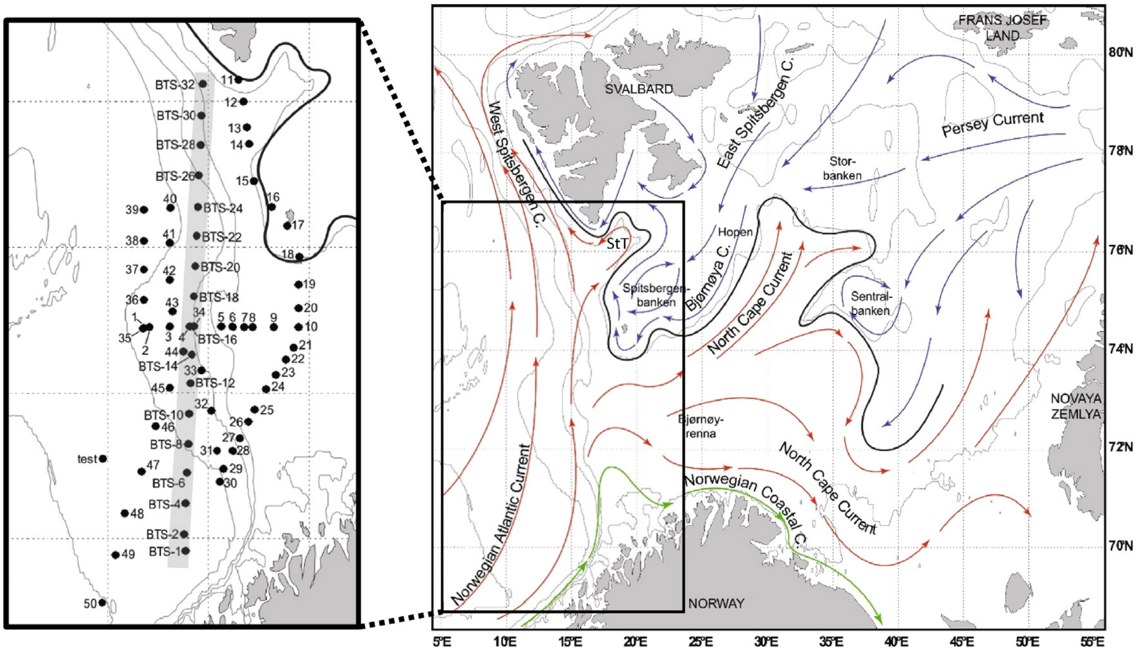

Fig. 1. Surface water circulation in the Barents Sea (after Solignac et al., 2009) and locations of the study area and coccolithophore sampling stations. The solid black line is the mean position of the Polar Front after Loeng (1991). Stations labeled "BTS" are part of the water column transect (gray rectangle) within the zoom box. All other labels correspond to underway surface water samples. StT: Storfjorden trough.

a SBE 38 thermosalinograph mounted near the ship's sea water inlet (−5 m) from August 15 to September 4, 2014. Additional SST and SSS records were taken from 32 CTD stations sampled from August 22 to 26, 2014, along a ca. 700 km long S–N water column transect (Fig. 1, Suppl. Table A1). The resulting 82 coupled SST and SSS data were spatially interpolated (gridding) according to the DIVA application (Troupin et al., 2012) of the Ocean Data View program (Schlitzer, 2014) in order to highlight the mean signature and spatial distribution of the main water masses and hydrological fronts during the ca. 19 days of water sampling. Surface water Chl *a* concentrations (mg/m^3) and PIC data (mol/m^3) were extracted under ArcGIS (©) at the location of each coccolithophore sampling station from MODIS Aqua 4 km resolution, 16 days (Aug. 21–Sept. 6, 2014) composite images obtained from the Giovanni application developed by GES DISC (http://disc.sci.gsfc.nasa.gov/giovanni).

The water column distributions of temperatures, salinity, sigma-t, and Chl *a* were obtained from the 32 vertical casts deployed along the S–N transect, from 0 to 600 m water depth. Vertical profiles of temperature and salinity were measured using a CTD SBE 9 plus. The fluorescence data obtained using a CHELSEA (©) fluorimeter mounted on the CTD frame were converted into Chl *a* concentrations (mg/m^3) based on a calibration curve constructed after shore-based HPLC analyses of 2 to 4 shallow water samples (top 25 m) per station. All data were thereafter plotted using the same interpolation procedure used for surface water parameters (DIVA gridding). The depth of the upper mixed layer (here referred as Mixed Layer Depth — MLD) was determined from each CTD profile according to Poulton et al. (2010) as the first depth where sigma-t values exceeded 0.05 per meter.

3.2. Phytoplankton data

3.2.1. Coccolithophores

Coccolithophore investigation was conducted on a set of 50 underway surface samples taken from the ship's sea water inlet, as well on water column samples collected along the S–N transect. Water column coccolithophore samples were collected at 17 out of the 32 CTD stations by way of Niskin bottles at fixed water depths of surface (2–3 m), 20 m, 50 m, 70 m, 100 m and 200 m (Fig. 1, Suppl. Tables A1, A2). Coccolithophore sampling involved onboard membrane filtration (pore size 0.8 μm) of 3 to 4 L of sea water as described by Andruleit (1996). Filters were subsequently air-dried and stored in Petri-dishes. In the laboratory, a ca. 20 mm^2 of the filter was cut out and mounted in 2–3 drops of immersion oil between slide and cover-slip for examination under a light microscope (LM) at ×1200 magnification, as described by Giraudeau et al. (1993). A total of 152 samples were investigated for both coccosphere (cells) and coccolith (liths) abundance (Suppl. Tables A1, A2) and the results expressed as cell and lith concentrations (number/ml) considering the volume of filtered sea water and the surface of the filter effectively analyzed under LM for coccolithophore abundance (see review by Giraudeau and Beaufort, 2007). A minimum of 200 cells and 500 liths were routinely identified and counted at species or genus levels. Rare taxa accounting for less than 0.5% of the total coccolithophore (cells or liths) populations were recorded as present or absent based on LM screening of ca. 50 additional view-fields. Based on the distributional maps and datasets of bulk cell and lith abundances (Figs. 5a and 6a, Suppl. Table A1), coccolithophore sampling using the sea water inlet did not induce obvious mechanical stress leading to artificial increases of the bulk lith to cell ratio compared with sampling using the CTD casts. Scanning electron microscope (SEM) observations were conducted on a limited (×10) set of surface and water column samples in order to verify the coccolithophore taxonomy inferred from LM observations. With the exception of a few extremely rare additional taxa, the SEM observations confirmed the species and/or genus level identifications by LM. Taxonomical concepts used in this study are based essentially on Young et al. (2003), Frada et al. (2010) and Young et al. (2015).

Coccolith calcite expressed in mol C/m^3 was calculated after Young and Ziveri (2000) and Beaufort and Heussner (1999), from the cell and lith concentration data within each surface water sample, based on estimates of lith species-specific morphology and size, and the average number of liths per cell. Coccolith calcite was calculated from the concentrations of the overwhelmingly dominant species *E. huxleyi* and of the highly calcified and common heterococcolith form of *Coccolithus pelagicus* ssp. *pelagicus* (hereafter named *C. pelagicus*) only. Average $CaCO_3$ weights of 2.3 pg and 398.6 pg for individual liths of *E. huxleyi* (mean length = 3.5 μm) and *C. pelagicus* (mean length > 11 μm), respectively, as well as an average of 20 liths/cell (*E. huxleyi*) and 18 liths/cell (*C. pelagicus*) were used to estimate coccolith calcite in each investigated surface water sample. Coccolith calcite values were then compared to remote sensing derived values of surface water PIC.

3.2.2. Phytoplankton pigments

The phytoplankton community structure during the sampling period, including the contribution of coccolithophores to the bulk phytoplankton biomass, was assessed from measurements of chlorophyll and carotenoid marker pigments in a limited set (7 stations) of both surface (2–3 m) and subsurface (20 m) samples collected evenly as part of the S–N water column transect of 32 CTD casts. One liter of water collected by way of Niskin bottles was passed through a sieve of 200 μm mesh size to remove meso- and macrozooplankton before filtration onto glass fiber filters and storage in liquid nitrogen at −196 °C until analysis. Shore-based analyses involved HPLC-based separation of marker pigments following the method of Van Heukelem and Thomas (2001). Phytoplankton class abundances were derived from the application of the CHEMTAX program (Mackey et al., 1996). The pigments used for the analysis were the same as used in similar Arctic environments such as the Baffin Bay (Vidussi et al., 2004) and the western Arctic Ocean (Fujiwara et al., 2014): Chl *a*, Chlorophyll *b* (Chl *b*), Chlorophyll *c3* (Chl *c3*), Peridinin (Peri), 19′-Butanoyloxyfucoxanthin (But), Fucoxanthin (Fuco), 19′-Hexanoyloxyfucoxanthin (Hex), Alloxanthin (Allo), Zeaxanthin (Zea), Lutein (Lut), and Prasinoxanthin (Pras). The definition of algal classes and corresponding specific accessory pigments for our study area, as well as the initial CHEMTAX pigment/Chl *a* ratios were taken from Vidussi et al. (2004). The pigment ratio for cyanobacteria, an algal group absent from the Baffin Bay dataset of Vidussi et al. (2004) was taken from Gibb et al. (2001). The algal groups and marker pigments, as well as the final CHEMTAX results on accessory pigment/Chl *a* ratios are given in Table 1. The subdivision of prymnesiophytes into two sub-groups is based on differences in the Hex/Chl *a* ratios as well as the presence/absence of But in the pigment signatures. According to the most abundant species identified in the present study (see Section 4), as well as the species-specific pigment signature of coccolithophores (Van Lenning et al., 2004), we ranged coccolithophores into either subgroups (e.g. *E. huxleyi* into Prymnesiophytes 1; *C. pelagicus* into Prymnesiophytes 2). The non coccolith bearing prymnesiophyte *Phaeocystis pouchetii*, an often dominant species in the phytoplankton community of the well mixed, Atlantic water-influenced surface waters of the southern and central Barents Sea (Reigstad et al., 2002) was ranged into the Fuco-flagellate group according to its specific high Fuco/Chl *a* ratio and absence or trace amounts of Hex and But (Vaulot et al., 1994).

4. Results and discussion

4.1. Hydrological context

The distributional patterns of SSTs and SSSs measured at each underway and CTD coccolithophore sampling location are given in Fig. 2. Three surface water masses can be characterized based on their temperature and salinity values according to Loeng (1991). They are linked to the main current systems over the western Barents Sea and the eastern

Table 1
Phytoplankton groups and final accessory pigments/Chl a ratio (g/g) calculated from CHEMTAX. Subgroups and initial ratios are taken from Vidussi et al. (2004), and Gibb et al. (2001) — see Section 3.

Phytoplankton group	Chl-c3	Peri	But	Fuco	Hex	Allo	Zea	Lut	Chl-b	Prasino
Prasinophytes 1	0	0	0	0	0	0	0	0	0.899	0.101
Prasinophytes 2	0	0	0	0	0	0	0.013	0.002	1.001	0
Cyanobacteria	0	0	0	0	0	0	0.716	0	0	0
Chlorophytes	0	0	0	0	0	0	0.103	0.254	0.083	0
Dinoflagellates	0	0.544	0	0	0	0	0	0	0	0
Cryptophytes	0	0	0	0	0	0.687	0	0	0	0
Prymnesiophytes 1	0.007	0	0	0.091	2.066	0	0	0	0	0
Prymnesiophytes 2	1.049	0	0.012	0.503	0.035	0	0	0	0	0
Chrysophytes + Pelagophytes	0.031	0	1.584	0.371	0	0	0	0	0	0
Fuco-flagellates	0	0	0	0.088	0	0	0	0	0	0
Diatoms	0	0	0	1.329	0	0	0	0	0	0

Norwegian Sea. Norwegian Atlantic Water (NwAW) defined by salinity >35.0 flows over the Barents Sea deep slope and penetrates into the Barents Sea over the Storfjorden and Bjørnøyrenna troughs. The surface expression of NwAW over the latter trough is separated from its main tributary by a limb of lower salinity water (34.7–35.0) of mixed NwAW–Norwegian Coastal Water (NwCW) which extends in a

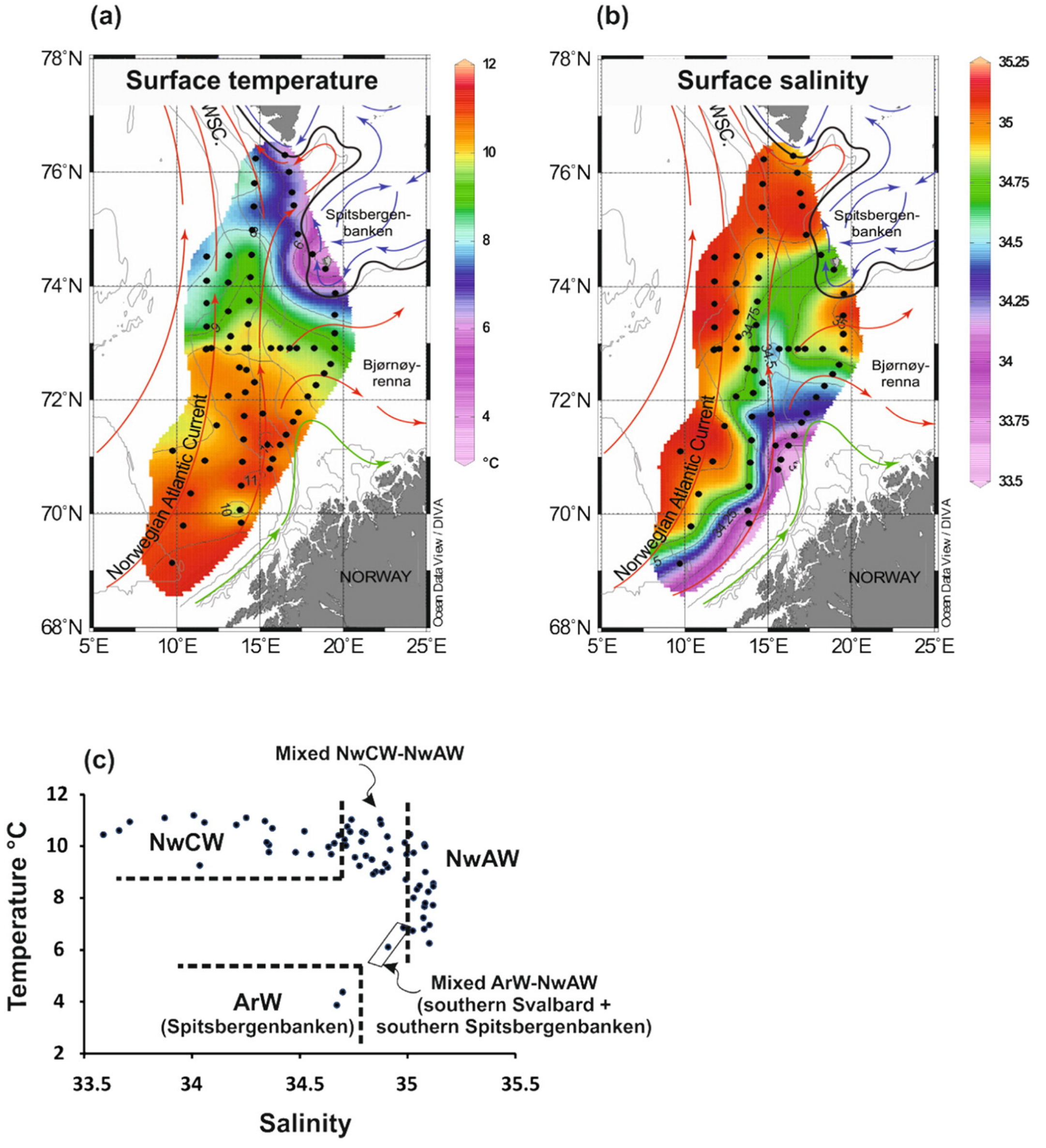

Fig. 2. Surface temperature, salinity and Chl *a* during August–September 2014. Black dots: sampling stations. (a) and (b): spatial interpolation (DIVA gridding) of underway measurements of SSTs and SSSs, respectively. (c): TS diagram with mean signatures of the surface water masses after Blindheim and Loeng (1981); NwCW: Norwegian Coastal Water, NwAW: Norwegian Atlantic Water, ArW: Arctic Water.

northern direction along the shelf break up to ca. 75°N as well as eastward into the Barents Sea following the path of the NCC. The NwCW with typical low salinity signature (<34.7) spreads out far from the core of the Norwegian Coastal Current (NwCC) as expected from the summer maximum seaward extent of this coastal water (Blindheim and Loeng, 1981). Cool (<5 °C) and low salinity (<34.8) Arctic Water (ArW) lays over the Spitbergenbanken in close vicinity to Bjørnøya Island. Mixed ArW–NwAW was sampled on two occasions in the northern tip of the studied area, close to southern Svalbard, as well as south of Bjørnøya Island. The distribution of surface water masses during August–September 2014 (Fig. 2a and b) implies that most surface water sampling for coccolithophore investigations as part of the present study took place within NwCW, NwAW and mixed NwCW–NwAW (Fig. 2c).

The S–N along-slope water column transect of 32 CTD casts (Fig. 1) crossed the three above mentioned surface water masses. Temperature and salinity depth profiles plotted in Fig. 3a and b are limited to the top 220 m, i.e. to the range of water depth where coccolithophore sampling was conducted. NwAW occupies most part of this depth range, with the exception of the upper mixed layer in the south of 74.5°N. There, a buoyant, warm and low salinity surface layer made of NwCW and mixed NwCW–NwAW is separated from the Atlantic water mass by a well-defined pycnocline slightly oscillating around 25 m (Fig. 3c). NwAW reaches the surface of the transect north of 74.5°N where the combination of coolish (<8 °C) and saline (≥35.0) water reduces stratification and results in an homogenous, well mixed water column. A low temperature (<2 °C) and medium salinity (≈35.0) bottom water mass

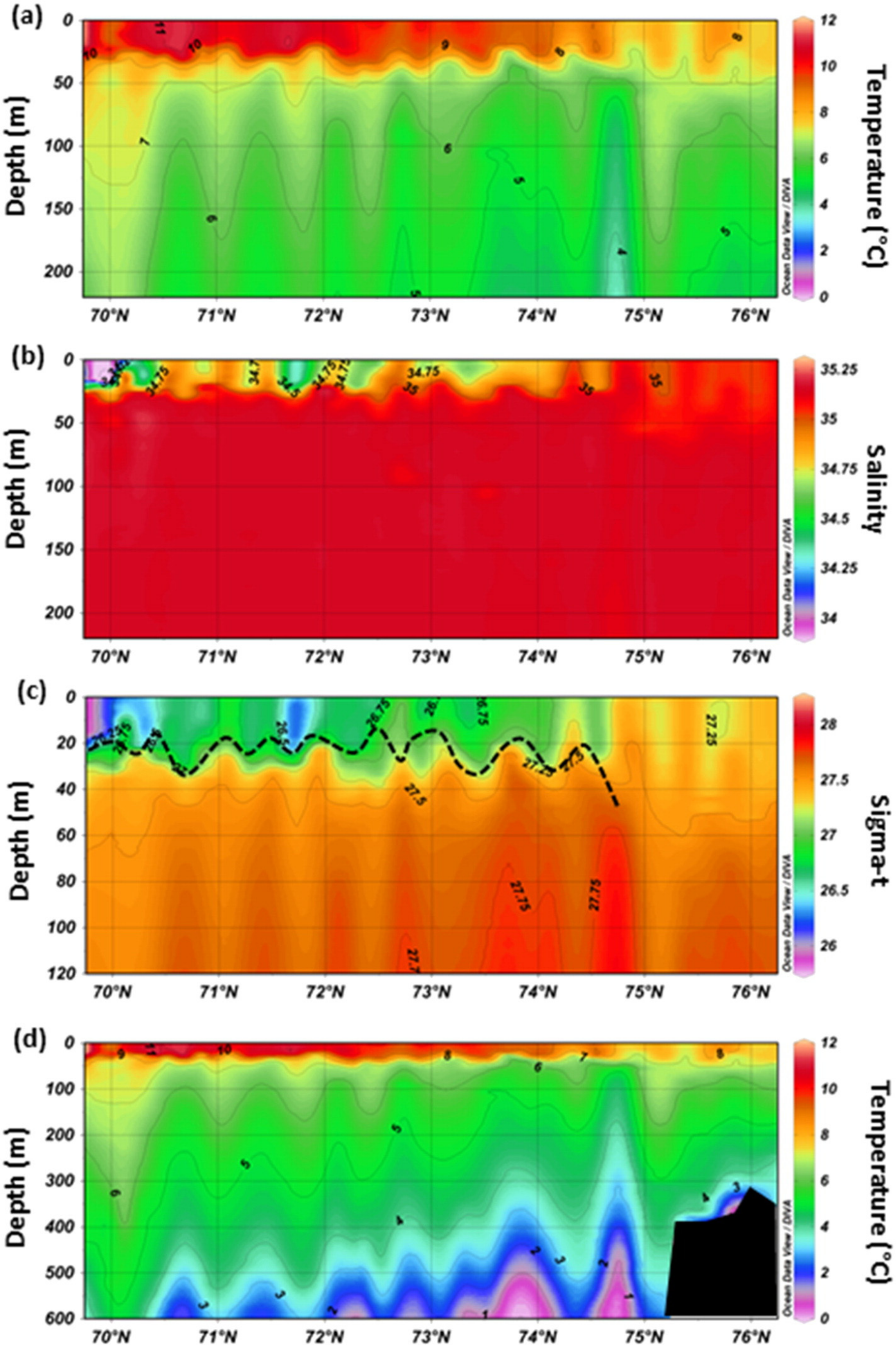

Fig. 3. Temperature (a and d), salinity (b) and density (sigma-t; c) in the water-column transect of BTS stations. Note the different depth scales used according to the features discussed in the text. Dotted line in the sigma-t plot: mixed layer depth. Black area in the bottom temperature plot: shelf break abutment north of 75°N.

occupies the deeper part of the CTD casts from ca. 450 m (Fig. 3d). This deep water mass bears characteristics of the Barents Sea Bottom Water which is formed in the Barents Sea and cascades down the slope to intermediate depths (500–800 m) in the Norwegian Sea (Blindheim, 1989). Both this water mass and the overlying NwAW are affected by increasingly higher amplitude shifts in temperature (Fig. 3c) and density (not shown) from 70.5°N (lower slope) to ca. 75°N (upper slope). These internal waves, which are here attributed to the interaction of the barotropic tide with the changing bathymetry in the vicinity of the Barents Sea slope and shelf break, show amplitudes ranging from 50 m in the south to 150 m in the northern part of the transect. Internal waves generated over shelf edges and continental slopes are common features of low to high latitudes continental margins (e.g. Helfrich and Melville, 2006). The present observation over the slope of the western Barents Sea might refer to other evidences of high amplitude internal waves in the northern sector of the Barents Sea which are generated by bathymetric anomalies on the shelf east of Spitsbergen Island (Kurkina and Talipova, 2011).

4.2. Phytoplankton pigments

The remote sensing-derived phytoplankton biomass in the surface waters of the study area, as expressed by Chl *a* concentrations (Fig. 4c), ranges from ca. 0.3 to 1.5 mg/m^3 (mean 0.8 mg/m^3), i.e. close to the average (2002–2008) August value of 0.7 mg/m^3 derived by Signorini and McClain (2009) for the wider southern-central Barents Sea. While lacking

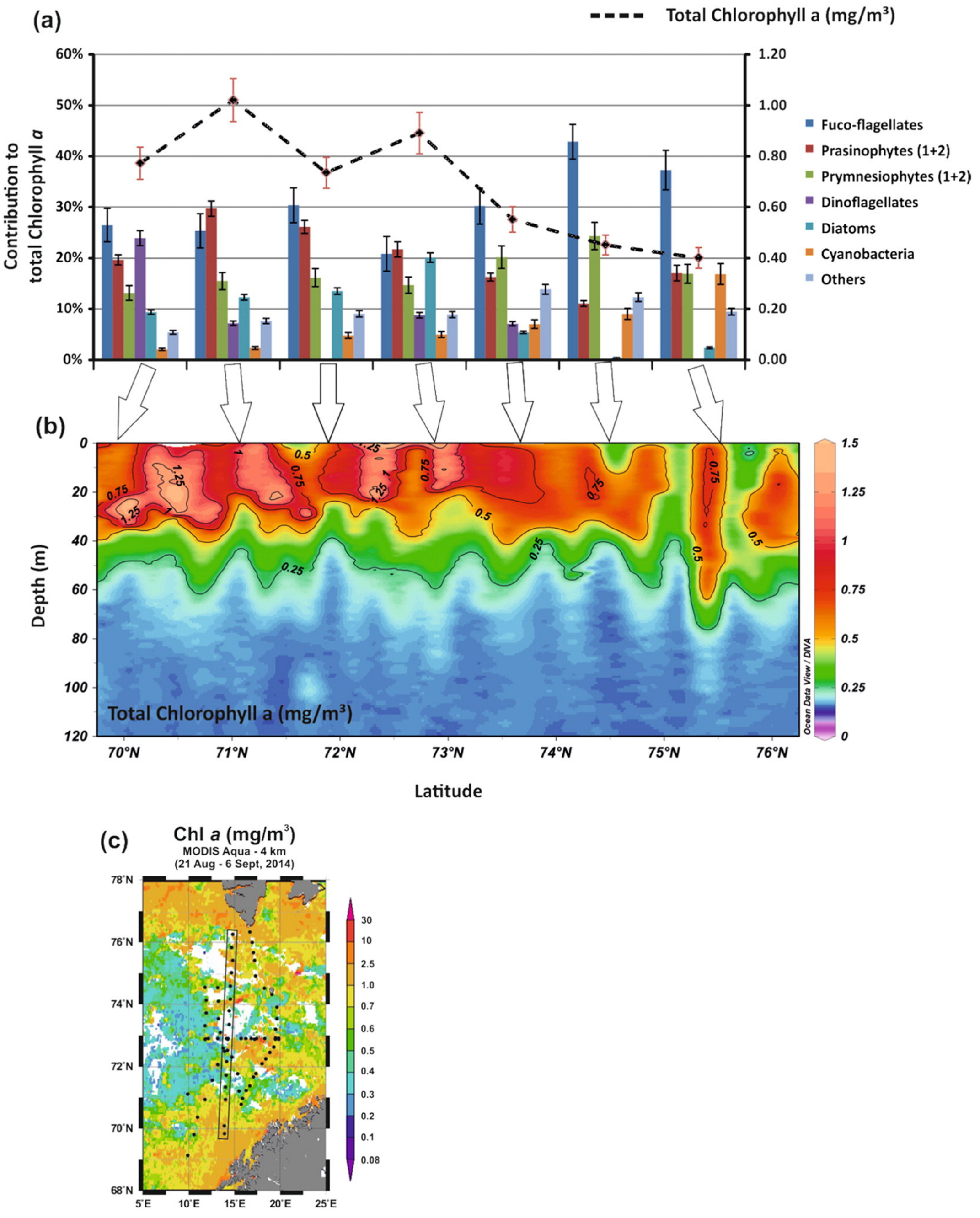

Fig. 4. (a and b): Vertical distribution of Chl *a* in the water column transect based on CTD fluorescence data (bottom plot), and contributions of the various algal groups to the total phytoplankton biomass in surface waters based on the analyses of accessory marker pigments (top plot). The locations of the surface water samples used for the pigment analyses are given by the empty arrows on top of the Chl *a* water column section. (c) Composite MODIS Aqua image (4 km resolution; August 21–September 6, 2014) of Chl *a* concentrations in surface waters of the studied area. Black empty rectangle: location of the transect of CTD casts.

a straightforward distributional pattern, surface Chl *a* shows higher values within NwCW as well as north of 76°N around Svalbard. The core of the NwAW to the west of 15°E is characterized by low Chl *a* values of ca. 0.2–0.4 mg/m^3 (Fig. 4c). The dynamical central domain of mixed NwAW–NwCW displays a very erratic pattern of surface Chl *a* distribution, with no relation to the general surface water circulation features (Fig. 1) and/or water mass distribution (Fig. 2b).

Depth profiles of Chl *a* concentrations measured along the S–N transect of CTD stations are shown in Fig. 4b. Chl *a* concentrations range from 0.3 to 1.3 mg/m^3 within the upper mixed layer. Highest values characterize the southern domain of mixed NwCW–NwAW south of 74°N, and are concentrated in the top 30 to 25 m of the water column above the well-developed pycnocline (Fig. 3c). The well mixed northern sector displays lower Chl *a* contents (<0.75 mg/m^3), moderate to high values occasionally reaching deeper water depths down to ca. 60 m. Such a deep chlorophyll maximum north of 75°N most probably results from the sinking, within a poorly stratified upper water column, of an earlier production event in surface waters.

The community structure along the S–N transect, as inferred from pigment analysis (Fig. 4a) of surface water samples is characterized by three small-sized algal groups: Fuco-flagellates, Prasinophytes and Prymnesiophytes. Fuco-flagellates contribute on average 30% to the total Chl *a* along the transect, with maximum abundances in well mixed NwAW north of 74°N. This dominance is likely related to the success of *P. pouchetii*, a colonial species which is responsible for important blooms in the Barents Sea during summer (Wassmann et al., 1990). The second most abundant contribution to the total Chl *a* is from the Prasinophyte group whose main autotrophic species *Micromonas pusilla* and *Bathycoccus pusilla* are major components of the picophytoplanktonic community in the high boreal latitudes including the Barents Sea (Lovejoy et al., 2007; Not et al., 2005). Prymnesiophytes, which here are mainly represented by type 1 and their characteristic species *E. huxleyi* (see Section 3) contribute from 13 to 24% to the total Chl *a*. Higher contributions are found in the northern part of the investigated transect (from 74°N) where total Chl *a* concentrations are relatively low (ca. 0.5 mg/m^3). Diatoms which, together with flagellates, explain most of the new production during spring in the southern and central Barents Sea (Wassmann et al., 1999; Signorini and McClain, 2009), have a limited contribution (5–20%) to the August 2014 phytoplankton community along our studied transect. Maximum relative abundances are reached in the southern NwCC-influenced region where nutrient delivery (among which silicon) from the coastal domain presumably supports their post spring-bloom outlasting. The above-described structure of the phytoplankton community inferred from the abundance of accessory pigments in surface water samples only (Fig. 4a) can be extended to deeper part of the upper photic layer along the Barents Sea shelf break and slope: HPLC analyses of water samples collected at the same CTD stations but deeper in the upper mixed layer (20 m) revealed a very similar distribution and contribution of the various algal groups to the total Chl *a* concentrations (Suppl. Table A3).

4.3. Surface and water column distribution of coccolithophores

Fifteen coccolithophore taxa were identified in our surface and water column samples (Table 2). Four species occurred only very occasionally and were not enumerated, and 6 taxa were only found as liths (no cells). Six surface water samples were barren of both cells and liths. Census counts of the 9 most abundant taxa (cells and/or liths) are given in Supplementary Tables A1 and A2.

Table 2
List of coccolithophore species identified in the studied set of surface and water column samples. Names followed by an asterisk refer to rare species whose liths and/or cells were too sporadically encountered to be enumerated. Also provided are information on the microscope method(s) of identification (LM and/or SEM), as well as on species only found as liths (X).

Coccolithophore taxa	Observation	Liths only
Acanthoica quatrospina	LM, SEM	
*Braarudosphaera bigelowii**	LM	
Algirosphaera robusta	LM, SEM	
*Calciopappus caudatus**	SEM	
Calcidiscus leptoporus	LM	X
Coccolithus pelagicus ssp. pelagicus HET	LM, SEM	
Coccolithus pelagicus ssp. pelagicus HOL	LM, SEM	
Emiliania huxleyi	LM, SEM	
Gephyrocapsa muellerae	LM, SEM	X
Gephyrocapsa oceanica	LM	X
Helicosphaera carteri	LM	X
*Pseudoemiliania lacunosa**	LM	X
*Syracosphaera marginaporata**	SEM	
Syracosphaera molischii	LM, SEM	
Small *Gephyrocapsa*	LM, SEM	X

4.3.1. Surface water distribution and contribution to PIC concentrations

Coccolithophores identified in surface water samples are overwhelmingly dominated by *E. huxleyi* which contributes an average of >90% to the bulk cell and lith assemblages. Rare exceptions concern 3 samples collected within cold, well mixed NwAW or mixed ArW–NwAW, both off southern Svalbard where dominance is equally shared with, if not taken by *C. pelagicus* cells and liths Fig. 5b). The location of this dominance shift during August 2014 can be considered as a rather long-standing pattern of summer coccolithophore species distribution in the western Barents Sea and eastern Greenland Sea, when compared with the 1987–1992 coccolithophore survey conducted within the Nordic Seas by Samtleben et al. (1995). Total coccolithophore cell concentrations average 30 cells/ml (Fig. 5a, Table A1) when excluding peak bloom concentrations off northern Spitsbergenbanken, and stand within the range of the few available standing stock values measured for the summer high production period of coccolithophores in the western Barents Sea, northeastern Norwegian Sea and eastern Greenland Sea (Samtleben et al., 1995; Baumann et al., 2000; Dylmer et al., 2015).

Our high (spatial) resolution set of surface water samples displays two distinct areas of maximum (>40 cells/ml) cell concentrations (Fig. 5a and c): medium to high standing stocks are found within NwCW as well as within the warmest, southern part of the mixed NwCW–NwAW domain, on one hand; cold NwAW immediately south and north of the ArW-bearing Spitsbergenbanken host the highest cell concentrations of 100 to >4000 cells/ml, on the other hand. Bloom conditions characterize the later area above the mouth of the Storfjorden trough. Lowest coccolithophore standing stocks are observed in the northwestern, NwAW-bathed part of the study area, north of 73°N, as well as within cool mixed NwCW–NwAW at the entrance of the Bjørnøyrenna trough. The above-mentioned domains of medium to high coccolithophore cell abundances (Fig. 5c) represent distinct coccolithophore communities and take place in drastically different mixed layer conditions. Cells of *E. huxleyi* identified in the two populations are of similar size (3–5 μm) and belong to the same variety, the A group of Young and Westbroek (1991). The assemblages are however different with regard to the abundance of the cold-water adapted species *C. pelagicus* (Samtleben and Schröder, 1992) which contributes significantly to the high standing stocks in the northeastern part of the study area, north and south of Spitsbergenbanken (Fig. 5b). The medium to high standing stock population found in the NwCW-influenced domain takes place in buoyant warm and low salinity water (Fig. 2) above a well-developed shallow pycnocline (Fig. 3). Such an environment is classically described as optimal for the summer development of *E. huxleyi* in the Nordic Seas (Samtleben et al., 1995; Baumann et al., 2000). Drastically different mixed layer conditions characterize the northeastern locus of peak coccolithophore cell concentrations above the Storfjorden trough where a bloom of *E. huxleyi* is recorded. This bloom is suggested to take place within a poorly stratified upper mixed layer as indicated from the low SSTs (ca. 6 °C) and high SSSs (35.10) measured at the sampling stations (Fig. 2, Supp. Table A1), as well as in view of the nearby S–N water column transect located to

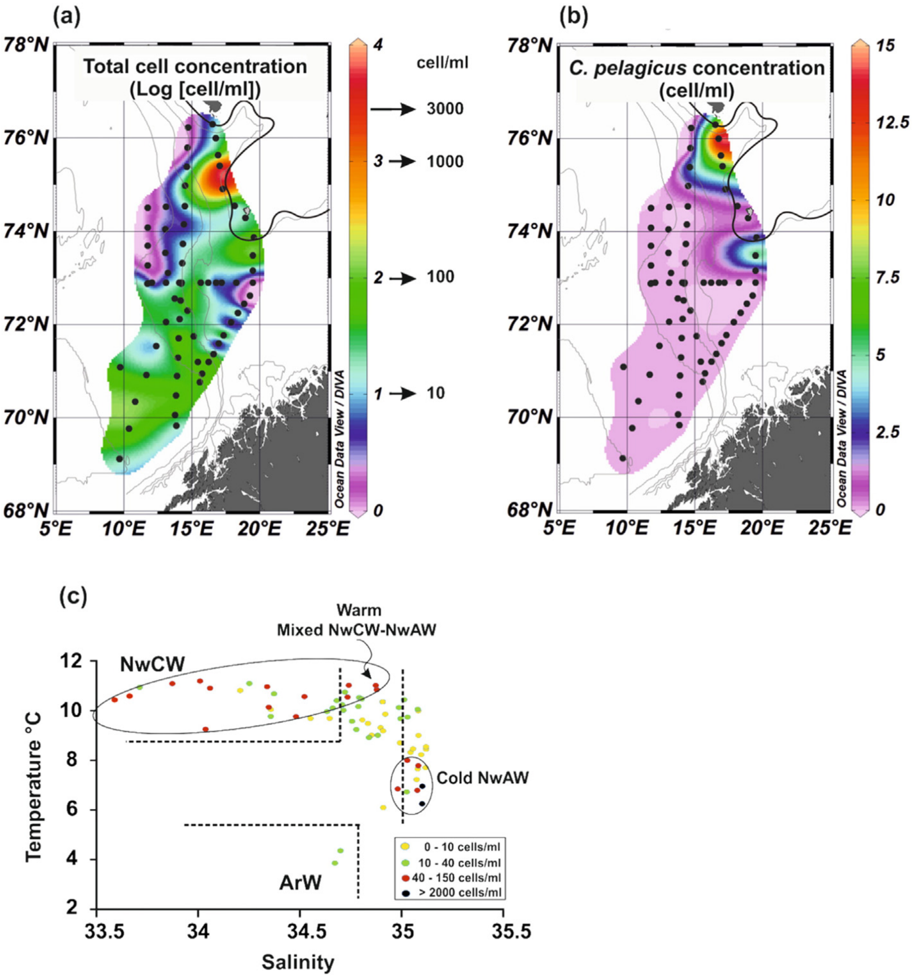

Fig. 5. Surface water distribution of coccolithophore cells. (a) Total coccolithophore concentrations (Log-transformed values). (b) *Coccolithus pelagicus* cell concentrations. (c) Distribution of total coccolithophore standing stocks according to TS values measured at each sampling stations. The areas of medium to high cell concentrations (>40 cells/ml) are highlighted by two distinct ellipses.

the west of this area (Fig. 3). The absence of CTD casts within the core of the bloom obviously limits further conclusion on the key physico-chemical conditions associated with the observed high coccolithophore stocks. Our dataset however indicates that conditions triggering the August 2014 bloom off northern Bjørnøya Island seem unique in view of those characterizing the pervasive summer blooms of *E. huxleyi* in the southern and central Barents Sea which take place within a shallow (ca. 10 m.) and fresh (ca. 34.2) mixed layer (Signorini and McClain, 2009).

Liths identified within the surface water samples are overwhelmingly dominated by *E. huxleyi* (Supp. Table A1). The abundance of total liths within the surface water samples (Fig. 6a) follows very closely the distributional patterns displayed by the coccolithophore cells (Fig. 5a). Peak concentrations of ca. 20 × 10^3 liths/ml (*E. huxleyi*-derived only) characterize the bloom domain off northern Spitsbergenbanken. The cell concentrations of ca. 2000 to 4000 cells/ml measured within these surface water samples indicate that the *E. huxleyi* bloom collected in August 2014 was in a stationary phase which follows the growing phase when cells outnumber detached liths (Frada et al., 2010). At the scale of the whole study area, the abundances of bulk liths display a statistically significant correlation with the Log-transformed total cell concentrations (Fig. 6b). According to such a correlation, the concentrations of detached liths are positively related with exponentially increasing coccolithophore standing stocks. The various coccolithophore populations sampled within the westernmost sector of the Barents Sea during August 2014 were therefore characterized by a common development state.

Some liths identified in the studied set of phytoplankton samples were taxononomically related to species for which cells were not observed in any of the surface water (or water column) samples. These liths contribute on average to ca. 1% of the total lith assemblages and belong, in order of decreasing contribution, to the following taxa: small *Gephyrocapsa*, *Gephyrocapsa muellerae*, *Gephyrocapsa oceanica*, and *Calcidiscus leptoporus*. All four taxa are barely found nowadays as living cells in modern plankton communities of the Nordic Seas. Their common contribution as liths to the fossil assemblages in surface sediments of the eastern Nordic Seas (e.g. Samtleben et al., 1995) or to the settling particles collected in deep sediment traps of the Norwegian and Greenland Seas (Samtleben and Bickert, 1990; Andruleit, 1997) has been attributed to drifting with the poleward flow of surface to intermediate Atlantic water from the southern Norwegian Sea and temperate North Atlantic where these species are thriving (Samtleben and Schröder, 1992; Baumann et al., 2000; Giraudeau et al., 2010; Dylmer et al., 2015). This process is thought to explain the surface water distribution of the summed concentrations of these four taxa, hereafter referred to "Advected liths" (Fig. 6c), with maximum values along the flow of the NwAC as well as near the inception of the NCC into the Barents Sea (ca. 73°N).

Coccolithophore-derived particulate inorganic carbon concentrations in surface waters, hereafter referred to coccolith calcite, are shown in Fig. 7a. Not surprisingly given the overwhelming dominance of *E. huxleyi*, coccolith calcite is distributed according to the same patterns shown by the total standing stocks (Fig. 5a), with a mean average

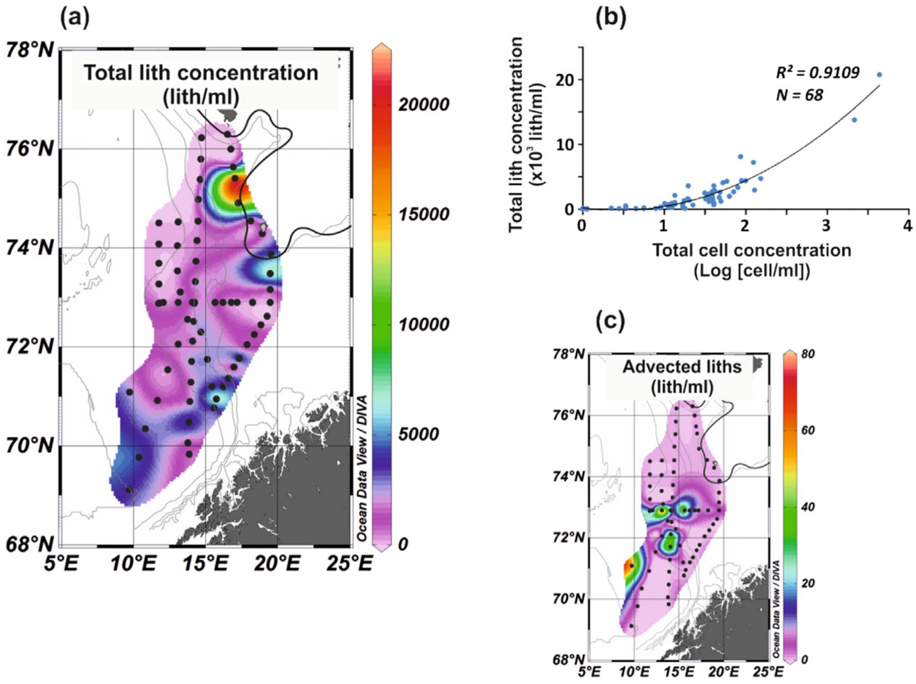

Fig. 6. Surface water distribution of detached coccolithophore liths. (a) Total lith concentrations. (b) Relationship between total cell and lith concentrations with 2nd degree polynomial regression (black curve). (c) Advected lith concentrations.

concentration of 0.2 mmol/m^3 over the whole studied area. *Maximum* coccolith calcite concentrations of 3.9 mmol/m^3 are estimated within the core of the *E. huxleyi* bloom off northern Spitsbergenbanken. This peak coccolith calcite value calculated from our cell and lith census counts (sample 14; see location in Fig. 1), corresponds to the PIC concentration of 3.95 mmol/m^3 extracted at the same sampling location from the remote sensing-derived data of total PIC (Fig. 7b), and indicates that the bulk surface water PIC in the bloom area is near exclusively contributed by coccolith calcite. Excluding the sample locations where bulk PIC values could not be extracted from the 16 days composite satellite map due to cloud cover (Fig. 7b), the mean bulk PIC concentrations are estimated as close to 1.8 mmol/m^3.

Fig. 7c displays the correlation between coccolith calcite and total PIC in non-bloom conditions (ie excluding samples 14 and 15) and excluding surface water samples barren of both cells and liths (see Suppl. Table A1). This plot indicates that additional sources of calcite, such as detrital carbonates, and other calcifying plankton organisms such as pteropods and foraminifera, contribute to a high extent to the total particulate inorganic carbon in surface waters. The statistically significant exponential relationship linking both datasets however suggests that, despite a large difference in mean values close to one order of magnitude (see above), coccolith calcite is involved into the observed variability of total calcite budget in non-bloom conditions, this influence being increasingly higher with higher coccolithophore stocks as indicated from the calculated coccolith contributions to surface water PIC (Fig. 7d). The relatively shallow and hydrologically dynamic setting of the studied area, as well as its proximity to continental Norway and the Svalbard archipelago, might at least partly explain the low mean contribution (ca. 20%) of coccolithophore-derived calcite to the total PIC in the surface water of the Barents Sea. This contribution is indeed in the lower range of rare measurements conducted during non-bloom situations in the North Atlantic, far from potential sources of detrital carbonates, where coccolith calcite is assumed to contribute to at least 40% of the total content of calcite in surface waters (Poulton et al., 2010).

4.3.2. Water column distribution

Bulk coccolithophore cells and liths display the same distributional pattern within the investigated S–N transect, with maximum density essentially concentrated in the top 20 m of the water column (Fig. 8a and b, Suppl. Table A2). Cell and lith densities are higher within the NwCW-influenced stratified upper mixed layer of the transect, peak concentrations of ca. 140 cells/ml and 3000 liths/ml, respectively, being found south of 71°N, within the flow of the NwCC. A deepening (down to 50 m) of peak coccolithophore abundances is observed, though very locally at ca. 75°N (Fig. 8a and b), in the northern part of the transect within the cold NwAW domain. This single, northern, deep high cell and lith density likely results from the sinking in poorly stratified upper waters, of the western limb of the *E. huxleyi* bloom identified in surface water samples off northern Spitsbergenbanken (Figs. 5a and 6a).

The pigment analysis conducted on a limited series of CTD stations (surface and 20 m water depth, see Section 4.2) is compared with cell enumerations at the same locations in order to test the robustness of the CHEMTAX-based coccolithophore biomass estimates (Fig. 8c). Despite the low amount of investigated stations (×7), the correlation (linear solution) between both datasets is statistically significant ($R^2 = 0.73$, p-value = 0.02) for the surface water samples, meaning that CHEMTAX reliably reproduces the changes in coccolithophore standing stocks within the upper part of the photic layer. This does not hold true for the deeper water layer (20 m) where no significant correlation can be inferred ($R^2 = 0.33$, p-value = 0.2). Changes in pigment/chl *a* ratios with depth are linked to changes in light availability and nutrient contents, together with changes in the physiological state of morphologically intact cells, a factor which is barely detectable from microscope observations of coccolithophores. They are common elements put forward in the literature to explain some limitations in the pigment-based calculation of algal class abundances (Jeffrey, 1981; Goericke and Montoya, 1998). Such changes in pigment ratios are likely to explain the observed poor correlation at depth between our chemical and microscope datasets (Fig. 8c), and call for extreme care when assessing algal community structure from marker pigments and/or cell enumeration only.

The species diversity of coccolithophore populations in the water column bears some similarities with the one described from the set of surface water samples distributed over the western shelf and slope of the Barents Sea (Section 4.3.1). The species *E. huxleyi* overwhelmingly

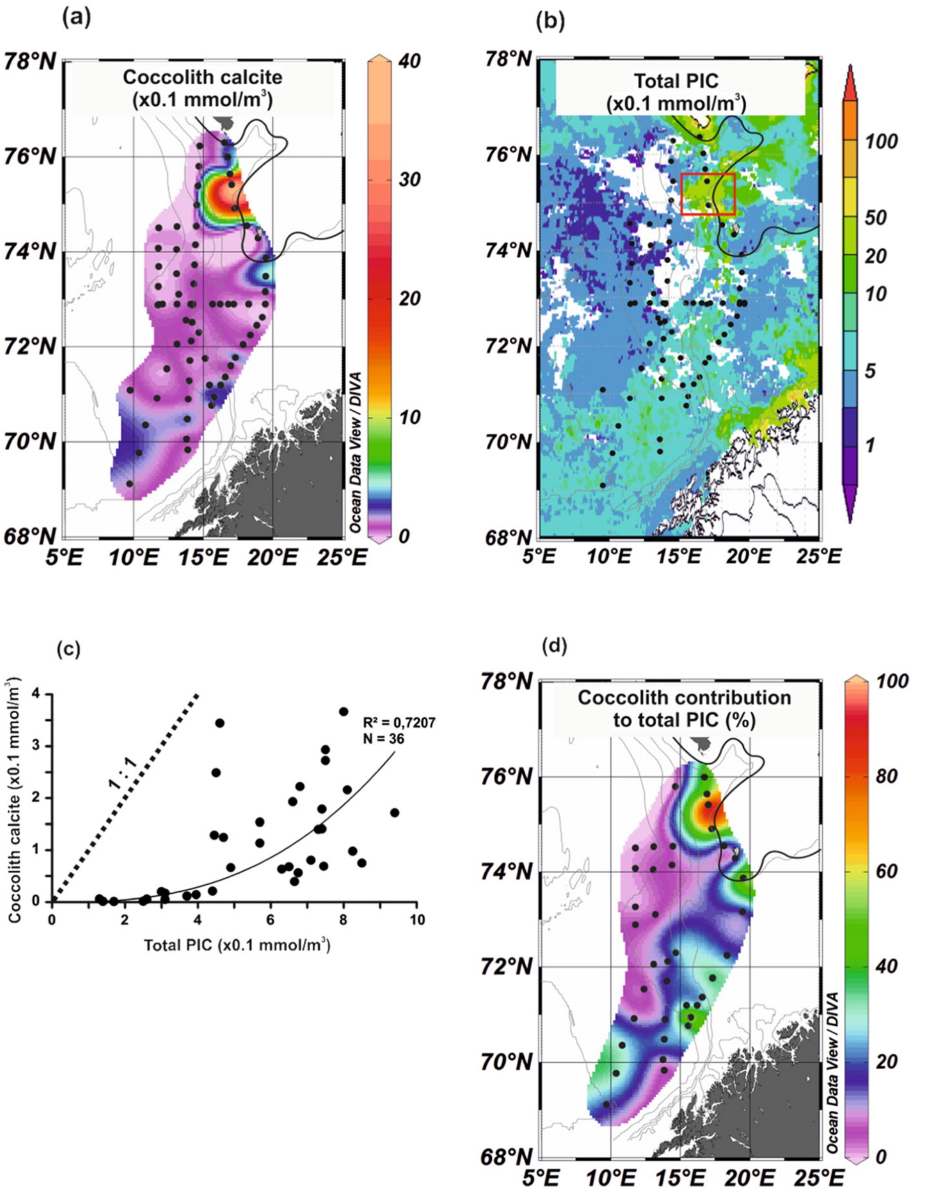

Fig. 7. Coccolith calcite in comparison with total PIC. (a) Coccolith calcite calculated from census counts of cells and liths. (b) Composite MODIS Aqua image (4 km resolution; August 21–September 6, 2014) of PIC concentrations. The red box highlights the location of maximum PIC concentration related to the *E. huxleyi* bloom. (c) Relationship between satellite-derived total PIC and coccolith calcite concentrations with 2nd degree polynomial regression (black curve). (d) Coccolith contribution to total PIC concentrations.

dominates both cell and lith assemblages (Fig. 8a and b, Suppl. Table A2), *C. pelagicus* being occasionally found as a subordinate species in the shallow to deepest part of the cool photic layer north of 74°N. Advected, exotic liths of small *Gephyrocapsa*, *G. muellerae*, *G. oceanica*, *C. leptoporus* and *Helicosphaera carteri*, the last species being only found here in the water-column samples, are essentially distributed in the shallow mixed layer south of 74°N (Fig. 8b) where the influence of warm mixed NwCC–NwAW is the strongest.

A unique coccolithophore distribution feature found during our water column survey lays in the high abundance of morphologically intact cells of *C. pelagicus* and *Algirosphaera robusta* in the deepest part of the investigated transect (i.e. 200 m water depth) (Fig. 8a), the last mentioned species being absent from the surface water algal community during the period of sampling. The species *A. robusta* is commonly observed in plankton communities of the Nordic Seas within mixed Atlantic–Arctic water mass, where it primarily inhabits deep layers below the thermocline (Samtleben and Schröder, 1992). Its fragile liths are hardly found in the water column and surface sediments, being rapidly altered after shedding. Medium concentrations of *A. robusta* of 2 to 4 cells/ml are found in the 20–70 m depth range of the studied transect (Fig. 8a), a depth interval which is likely to represent the main habitat of this species in the western Barents Sea during summer. Although also present in the upper mixed layer (Fig. 5b), *C. pelagicus* seems to adjust to a wider range of water-depth, as observed in previous water column surveys in the Norwegian and Greenland Seas (Samtleben and Schröder, 1992). The dominance of *C. pelagicus* in the coccolithophore populations (cells) collected at depth down to 60 m off eastern Greenland has also been tentatively related to its high resistance to alteration during sinking to deeper layers (Balestra et al., 2004). These two peculiarities, high range of light requirement and resistance to alteration, probably add to the poorly stratified conditions in the northern part of the transect to explain the observed mixed layer locus of *C. pelagicus* cell density at depth of ca. 50 m along the studied transect (Fig. 8a) particularly north of 74°N. Morphologically intact cells of both *A. robusta* and *C. pelagicus* are found in the deepest part of the investigated water column (200 m), with concentrations close to, if not higher than those found in the upper water layers (Fig. 8a). The sampling interval in the deeper part of the investigated depth interval (0–200 m) jumps from 100 to 200 m and therefore does

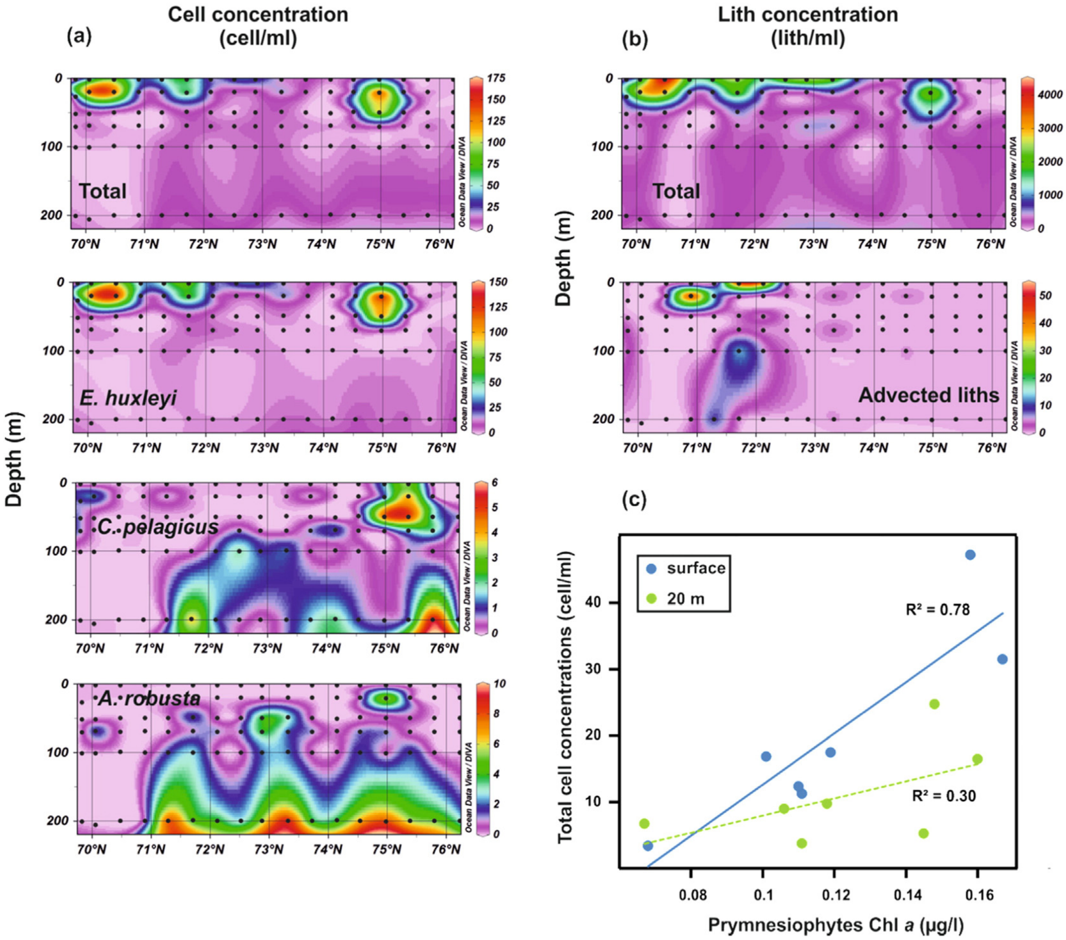

Fig. 8. Water column distribution of selected coccolithophore cells (a) and liths (b). (c) Comparison of cell counts with pigment-derived prymnesiophytes Chl *a* in surface waters (blue dots) and at 20 m water depth (green dots) from the 7 CTD stations identified in Fig. 4. Linear relationships and R^2 are also provided (blue: surface; green: 20 m).

not allow to assess more precisely the depth of this deep cell maxima nor its extent in the water column below 200 m. Profiles of photosynthetically available radiation (PAR) obtained as part of the CTD casts indicate that light levels below 100 m are well below 1% of the incident light and are not compatible with the production of strictly autotrophic phytoplankton organisms such as coccolithophores. Although recent works suggest that protists among which coccolithophore may develop a mixotrophic function during the final stage of their development (Rokitta et al., 2011; Mitra et al., 2014), the deep floral assemblage of intact coccospheres observed in the present study, which is almost exclusively made of the above-mentioned two taxa, must be seen as a relict assemblage of the extant population which once thrived in the lower photic layer. The mechanism of transfer to depth of this sinking population must be both quick, and non-biologically mediated (grazing) in order to preserve the morphologically fragile coccospheres of *A. robusta*. The low abundance of *E. huxleyi* cells at 200 m, with the exception of medium concentrations north of 74°N, compared with its abundances in surface waters (Fig. 8a) also suggests that this physical process does not affect the algal population from the upper photic layer above a well-defined pycnocline. Deep-living species, such as *A. robusta*, as well as taxa which thrive in the well-mixed photic layers of the northern sector of the studied transect are therefore able to sink rapidly to depth up to 200 m in the absence of strong vertical density gradient. High amplitude (up to 150 m) internal waves generated by the topography along the Barents Sea slope, whose roof reaches the pycnocline south of 74°N or the deep photic layers in well mixed upper waters north of this latitude (Fig. 3; Section 4.1), might be considered as an additional factor of vertical mixing and rapid transfer to depth of this sinking population.

5. Conclusions

The coccolithophore survey conducted in 2014 over the western Barents Sea shelf and slope during the high production period (summer) of this algal group took place outside the main region presently affected by recurring *E. huxleyi* blooms in the southern and central Barents Sea (Smyth et al., 2004; Signorini and McClain, 2009). The recorded standing stock values stand within the range of those typical of the nearby Norwegian and Greenland Seas for the same period of the year (Samtleben et al., 1995; Baumann et al., 2000; Dylmer et al., 2015). Our high spatial resolution study of surface and water column samples provides significant and unique information on the distribution of coccolithophore cells and liths within an hydrologically complex area. The present study can be summarized as follows:

(a) The coccolithophore population is characterized by a low species diversity, and the overwhelming dominance of both cells and liths of *E. huxleyi*. Calcareous prymnesiophytes contribute on average some 20% to the bulk Chl a in surface waters, as part of a summer phytoplankton community made essentially of small-sized algal groups. Medium to high coccolithophore standing stocks occupy two distinct environmental settings, one over a well stratified, NwCW-influenced shallow mixed layer, the other within well mixed cool NwAW in close vicinity of the Polar Front where concentrations reach bloom values (>4000 cells/ml) alike those usually recorded in the southern and central Barents Sea. Such a bimodal distribution of coccolithophore stocks, although made of different morphotypes, has been earlier shown in the temperate North Atlantic (Schiebel et al., 2011). Our observations suggest that subarctic to arctic populations of coccolithophores can successfully colonize a wide range of environmental conditions, and that the physical structure of the photic layer, an aspect which is often put forward to explain the timing of coccolithophore production as part of the seasonal phytoplankton succession, may not be the only key parameter at such high latitudes.

(b) Excluding the bloom situation, coccolith calcite accounts for some 20% of the bulk calcite content in surface waters, this contribution being increasingly higher with higher coccolithophore standing stocks. Detrital calcite, either made of reworked bottom shelf sediment or derived from the nearby continental Norway and Svalbard archipelago, is hypothesized as the most important contributor to the surface water PIC over the Barents Sea shelf and slope in non-bloom conditions. Our observations however suggest that the summer PIC values in the surface waters are statistically related, and therefore, to some extent, driven by changes in coccolith calcite concentrations.

(c) The presence in the deepest part of the investigated water column (200 m) of a unique assemblage of intact coccospheres gives evidence of the rapid transfer to depth of populations thriving in the deep photic zone below a well developed pycnocline, or within poorly stratified upper water layers. High amplitude internal waves generated over the Barents Sea slope by the interaction of the barotropic tide with the changing bathymetry might strengthen the vertical motion of rapidly sinking particles of the lower photic zone, among which intact coccospheres of deep water thriving coccolithophore species. This process must be viewed, together with other phenomena at play in this area such as the downslope cascading of reworked material associated with dense water masses and brines (Rumohr et al., 2001), as a key sedimentary process over the slope of the Western Barents Sea.

Acknowledgments

Thanks are due to the captain and crew of the SHOM MOCOSED 2014 cruise of the RV *Pourquoi Pas*? as well as the shipboard scientists from SHOM, Univ. Bordeaux and Univ. Angers for the successful sampling operations and the acquisition of oceanographic data. This work is a contribution to “The Changing Arctic and Subarctic Environment” (CASE) Initial Training Network funded by the European Community FP7, Marie Curie Actions, under Grant Agreement n°238111. We are grateful to Joëlle Salaun (SHOM) for the shore-based pigment analyses as well for her precious advices during the course of this investigation. Funding to Vivien Hulot was provided by SHOM under grant agreement 49/2015 "DYNSEDIM 2015". We thank the two anonymous referees as well as Eileen Hofmann, editor for JMS, for valuable comments.

Appendix A. Supplementary data

Supplementary data to this article can be found online at http://dx.doi.org/10.1016/j.jmarsys.2016.02.012.

References

Andruleit, H., 1996. A filtration technique for quantitative studies of coccoliths. Micropaleontology 42 (4), 403–406.

Andruleit, H., 1997. Coccolithophore fluxes in the Norwegian-Greenland Sea: seasonality and assemblage alterations. Mar. Micropaleontol. 31, 45–64.

Balestra, B., Ziveri, P., Monechi, S., Troelstra, S., 2004. Coccolithophorids from the Southeast Greenland margin (Northern North Atlantic): production, ecology and the surface sediment record. Micropaleontology 50 (1), 23–34.

Baumann, K.-H., Andruleit, H.A., Samtleben, C., 2000. Coccolithophores in the Nordic Seas: comparison of living communities with surface sediment assemblages. Deep-Sea Res. II 47, 1743–1772.

Beaufort, L., Heussner, S., 1999. Coccolithophorids on the continental slope of the Bay of Biscay — production, transport and contribution to mass fluxes. Deep-Sea Res. II 46, 2147–2174.

Blindheim, J., 1989. Cascading of Barents Sea bottom water into the Norwegian Sea. Rapp. P.-v. Réun. Cons. Int. Explor. Mer 188, 49–58.

Blindheim, J., Loeng, H., 1981. On the Variability of Atlantic influence in the Norwegian and Barents Seas. FiskDir. Skr. Ser. HavUnders 17 pp. 161–189.

Burenkov, V.I., Kopelevich, O.V., Rat'kova, T.N., Sheberstov, S.V., 2011. Satellite observations of the coccolithophorid bloom in the Barents Sea. Oceanology 51 (5), 766–774.

Dalpadado, P., Ingvaldsen, R.B., Stige, L.C., Bogstad, B., Knutsen, T., Ottersen, G., Ellertsen, B., 2012. Climate effects on Barents Sea ecosystem dynamics. ICES J. Mar. Sci. 69 (7), 1303–1316.

Dylmer, C.V., Giraudeau, J., Hanquiez, V., Husum, K., 2015. The coccolithophores *Emiliania huxleyi* and *Coccolithus pelagicus*: extant populations from the Norwegian-Iceland Seas and Fram Strait. Deep-Sea Res. I 98, 1–9.

Frada, M., Young, J., Cachão, M., Lino, S., Martins, A., Narciso, A., Probert, I., de Vargas, C., 2010. A guide to extant coccolithophores (Calcihaptophycidae, Haptophyta) using light microscopy. J. Nannoplankton Res. 31 (2), 58–112.

Fujiwara, A., Hirawake, T., Suzuki, K., Imai, I., Saitoh, S.-I., 2014. Timing of sea ice retreat can alter phytoplankton community structure in the Western Arctic Ocean. Biogeosciences 11, 1705–1716.

Gibb, S.W., Cummings, D.G., Irigoien, X., Barlow, R.G., Fauzi, R., Mantoura, C., 2001. Phytoplankton pigment chemotaxonomy of the northeastern Atlantic. Deep-Sea Res. II 48 (4), 795–823.

Giraudeau, J., Beaufort, L., 2007. In: Hillaire-Marcel, C., de Vernal, A. (Eds.), Coccolithophorids: From Extant Populations to Fossil AssemblagesProxies in Late Cenozoic Paleoceanography, Developments in Marine Geology *vol. 1*. Elsevier. http://dx.doi.org/10.1016/S1572-5480(07)01015–9.

Giraudeau, J., Monteiro, P.S., Nikodemus, K., 1993. Distribution and malformation of living coccolithophores in the Northern Benguela upwelling system off Namibia. Mar. Micropaleontol. 22, 93–110.

Giraudeau, J., Grelaud, M., Solignac, S., Andrews, J.T., Moros, M., Jansen, E., 2010. Millenial-scale variability in Atlantic water advection to the Nordic Seas derived from Holocene coccolith concentration records. Quat. Sci. Rev. 29, 1276–1287.

Goericke, R., Montoya, J.P., 1998. Estimating the contribution of microalgal taxa to chlorophyll a in the field — variations of pigment ratios under nutrient- and light-limited growth. Mar. Ecol. Prog. Ser. 169, 97–112.

Hegseth, E.N., Sundfjord, A., 2008. Intrusion and blooming of Atlantic phytoplankton species in the high Arctic. J. Mar. Syst. 74, 108–119.

Helfrich, K.R., Melville, W.K., 2006. Long nonlinear internal waves. Annu. Rev. Fluid Mech. 38, 395–425.

Hovland, E.K., Hancke, K., Alver, M.O., Drinkwater, K., Høkedal, J., Johnsen, G., Moline, M., Skshaug, E., 2014. Optical impact of an *Emiliania huxleyi* bloom in the frontal region of the Barents Sea. J. Mar. Syst. 130, 228–240.

Hunt Jr., G.L., Drinkwater, K.F., 2005. Ecosystem studies of sub-arctic seas (ESSAS) science plan. GLOBEC Report No.19. viii (60 pp.).

Jeffrey, S.W., 1981. Light quality and pigment adaptations in microalgae. Proceedings of the International Botanical Congress, p. 179.

Kurkina, O.E., Talipova, T.G., 2011. Huge internal waves in the vicinity of the Spitsbergen Island (Barents Sea). Nat. Hazards Earth Syst. Sci. 11, 981–986.

Loeng, H., 1991. Features of the physical oceanographic conditions of the Barents Sea. Polar Res. 10 (1), 5–18.

Lovejoy, C., Vincent, W.F., Bonilla, S., Roy, S., Martineau, M.J., Terrado, R., Potvin, M., Massana, R., Pedrós-Alió, C., 2007. Distribution, phylogeny, and growth of cold-adapted picoprasinophytes in arctic seas. J. Phycol. 43 (1), 78–89.

Mackey, M.D., Mackey, D.J., Higgins, H.W., Wright, S.W., 1996. CHEMTAX — a program for estimating class abundances from chemical markers: application to HPLC measurement of phytoplankton. Mar. Ecol. Prog. Ser. 144, 265–283.

Mitra, A., Flynn, K.J., Burkholder, J.M., Berge, T., Calbet, A., Raven, J.A., Granéli, E., Glibert, P.M., Hansen, P.J., Stoecker, D.K., Thingstad, F., Tillmann, U., Våge, S., Wilken, S., Zubkov, M.V., 2014. The role of mixotrophic protists in the biological carbon pump. Biogeosciences 11, 995–1005.

Not, F., Massana, R., Latasa, M., Marie, D., Colson, C., Eikrem, W., Pedrós-Alió, C., Vaulot, D., Simon, N., 2005. Late summer community composition and abundance of photosynthetic picoeukaryotes in Norwegian and Barents Seas. Limnol. Oceanogr. 50 (5), 1677–1686.

Ozhigin, V.K., Trofimov, A.G., Ivshin, V.A., 2000. The eastern basin water and currents in the Barents Sea. ICES Council Meeting Papers CM 2000/L:14 (19 pp.).

Poulton, A.J., Charalampopoulou, A., Young, J.R., Tarran, G.A., Lucas, M.I., Quartly, G.D., 2010. Coccolithophore dynamics in non-bloom conditions during late summer in the Central Iceland basin (July–August 2007). Limnol. Oceanogr. 55 (4), 1601–1613.

Reigstad, M., Wassmann, P., Wexels Riser, C., Øygarden, S., Rey, F., 2002. Variations in hydrography, nutrients and chlorophyll *a* in the marginal ice-zone and the Central Barents Sea. J. Mar. Syst. 38, 9–29.

Rokitta, S.D., de Nooijer, L.J., Trimborn, S., de Vargas, C., Rost, B., John, U., 2011. Transcriptome analyses reveal differential gene expression patterns between the life-cycle stages of *Emiliania huxleyi* (Haptophyta) and reflect specialization to different ecological niches. J. Phycol. 47 (4), 829–838.

Rumohr, J., Blaume, F., Erlenkeuser, H., Fohrmann, H., Hollender, F.-J., Mienert, J., Schäfer-Neth, C., 2001. Records and processes of near-bottom sediment transport along the Norwegian-Greenland Sea margins during Holocene and Late Wechselian (termination I) times. In: Schäfer, P., Ritzrau, W., Schlüter, M., Thiede, J. (Eds.), The Northern North Atlantic: A Changing Environment. Springer, Berlin, pp. 155–178 (2001).

Samtleben, C., Bickert, T., 1990. Coccoliths in sediment traps from the Norwegian Sea. Mar. Micropaleontol. 16, 39–64.

Samtleben, C., Schröder, 1992. Living coccolithophore communities in the Norwegian-Greenland Sea and their record in sediments. Mar. Micropaleontol. 19, 333–354.

Samtleben, C., Schaefer, P., Andruleit, H., Baumann, A., Baumann, K.-H., Kohly, A., Matthiessen, J., Schröder-Ritzrau, A., 1995. Plankton in the Norwegian-Greenland Sea: from living communities to sediment assemblages — an actualistic approach. Geol. Rundsch. 84, 108–136.

Schiebel, R., Brupbacher, U., Schmidtko, S., Nausch, G., Waniek, J.J., Thierstein, H.R., 2011. Spring coccolithophore production and dispersion in the temperate Eastern North Atlantic Ocean. J. Geophysical Res. 116, C08030.

Schlitzer, R., 2014. Ocean Data View. http://odv.awi.de (2014).

Signorini, S.R., McClain, C.R., 2009. Environmental factors controlling the Barents Sea spring–summer phytoplankton blooms. Geophys. Res. Lett. 36, L10604.

Smedsrud, L.H., Esau, I., Ingvaldsen, R.B., Eldevik, T., Haugan, P.M., Li, C., Lien, V.S., Olsen, A., Omar, A.M., Otterå, O.H., Risebrobakken, B., Sandø, A.B., Semenov, V.A., Sorokina, S.A., 2013. The role of the Barents Sea in the Arctic climate system. Rev. Geophys. 51. http://dx.doi.org/10.1002/rog.20017.

Smyth, T.J., Tyrrell, T., Tarrant, B., 2004. Time series of coccolithophore activity in the Barents Sea, from twenty years of satellite imagery. Geophys. Res. Lett. 31, L11302.

Solignac, S., Grøsfjeld, K., Giraudeau, J., de Vernal, A., 2009. Distribution of modern dinocyst assemblages in the Western Barents Sea. Nor. J. Geol. 89, 109–119.

Troupin, C., Barth, A., Sirjacobs, D., Ouberdous, M., Brankart, J.M., Brasseur, P., Beckers, J.M., 2012. Generation of analysis and consistent error fields using the data interpolating variational analysis (DIVA). Ocean Model. 52, 90–101.

Van Heukelem, L., Thomas, C.S., 2001. Computer-assisted high performance liquid chromatography method development with applications to the isolation and analysis of phytoplankton pigments. J. Chromatogr. 910, 31–49.

Van Lenning, K., Probert, I., Latasa, M., Estrada, M., Young, J.R., 2004. Pigment diversity of coccolithophores in relation to taxonomy, phylogeny and ecological preferences. In: Thierstein, H.R., Young, J.R. (Eds.), Coccolithophores. From Molecular processes to global impact. Springer, Verlag Berlin Heidelberg, pp. 51–73.

Vaulot, D., Birrien, J., Marie, D., Casotti, R., Veldhuis, M.J.W., Kraay, G.W., Chretiennot-Dinet, M.-J., 1994. Morphology, ploidy, pigment composition, and genome size of cultured strains *Phaeocystis* (Prymnesiophyceae). J. Phycol. 30, 1022–1035.

Vidussi, F., Roy, S., Lovejoy, C., Gammelgaard, M., Thomsen, H.A., Booth, B., Tremblay, J.-E., Mostajir, B., 2004. Spatial and temporal variability of the phytoplankton community structure in the North Water Polynya, investigated using pigment biomarkers. Can. J. Aquat. Sci. 61, 2038–2052.

Wassmann, P., Vernet, M., Mitchell, B.G., Rey, F., 1990. Mass sedimentation of *Phaeocystis pouchetii* in the Barents Sea. Mar. Ecol. Prog. Ser. 66, 183–195.

Wassmann, P., Ratkova, T., Andreassen, I., Vernet, M., Pedersen, G., Rey, F., 1999. Spring bloom development in the marginal ice zone and the Central Barents Sea. Mar. Ecol. 20 (3–4), 321–346.

Winter, A., Henderiks, J., Beaufort, L., Rickaby, R.E.M., Brown, C.W., 2014. Poleward expansion of the coccolithophore *Emiliania huxleyi*. J. Plankton Res. 36 (2), 316–325.

Young, J.R., Westbroek, P., 1991. Genotypic variation in the coccolithophorid species *Emiliania huxleyi*. Mar. Micropaleontol. 18, 5–23.

Young, J.R., Ziveri, P., 2000. Calculation of coccolith volume and its use in calibration of carbonate flux estimates. Deep-Sea Res. II 47 (9–11), 1679–1700.

Young, J.R., Geisen, M., Cros, L., Kleijne, A., Sprengel, C., Probert, I., Østergaard, J., 2003. A guide to extant coccolithophore taxonomy. J. Nannoplankton Res. Spec. Issue 1 (125 pp.).

Young, J.R., Bown, P.R., Lees, J.A., 2015. Nannotax3 Website. International Nannoplankton Association. (February URL: http://ina.tmsoc.org/Nannotax3).